Fungal Genetics and Biology 53 (2013) 84–96

Contents lists available at SciVerse ScienceDirect

Fungal Genetics and Biology

journal homepage: www.elsevier.com/locate/yfgbi

Eisosome distribution and localization in the meiotic progeny of *Aspergillus nidulans*

Alexandros Athanasopoulos [a], Haralabia Boleti [b], Claudio Scazzocchio [c,d], Vicky Sophianopoulou [a,*]

[a] Institute of Biosciences and Applications, Microbial Molecular Genetics Laboratory, National Center for Scientific Research, Demokritos (NCSRD), Athens, Greece
[b] Intracellular Parasitism Group, Molecular Parasitology Laboratory, Department of Microbiology and Light Microscopy Unit, Institute Pasteur Hellenique, Athens, Greece
[c] Department of Microbiology, Imperial College, London, United Kingdom
[d] Institut de Gènètique et Microbiologie, Université Paris-Sud, UMR8621 Orsay, France

ARTICLE INFO

Article history:
Received 1 November 2012
Accepted 10 January 2013
Available online 6 February 2013

Keywords:
Emericella
Eisosomes
Ascospore
Cleistothecium
Ascus
Sexual cycle

ABSTRACT

In the model filamentous fungus *Aspergillus nidulans*, PilA and PilB, two homologues of the *Saccharomyces cerevisiae* eisosome proteins Pil1/Lsp1, and SurG, a strict orthologue of Sur7, are assembled and form tightly packed structures in conidiospores. As *A. nidulans* differs in its reproduction pattern from the Saccharomycotina in that it has the ability to reproduce through two different types of spores, conidiospores and ascospores, the products of the asexual and the sexual cycle respectively, we investigated the eisosome distribution and localization during the sexual cycle. Our results show that core eisosome proteins PilA, PilB and SurG are not expressed in hülle cells or early ascospores, but are expressed in mature ascospores. All eisosomal proteins form punctate structures at the membrane of late ascospores. In mature but quiescent ascospores, PilA forms static punctate structures at the plasma membrane. PilB also was observed at the ascospore membrane as well, with higher concentration at the areas where the two halves of ascospores are joined together. Finally, SurG was localized both at the membrane of ascospores and perinuclearly. In germlings originating from ascospores the punctate structures were shown to be composed only of PilA. PilB is diffused in the cytoplasm and SurG was located in vacuoles and endosomes. This altered localization is identical to that found in germlings originated from conidiospores. In germinated ascospores PilA foci did not colocalise with the highly mobile and transient peripheral punctate structures of AbpA, a marker for sites of clathrin-mediated endocytosis. Deletions of each one or all the three core eisosomal genes do not affect viability or germination of ascospores. In the presence of myriocin – a specific inhibitor of sphingolipid biosynthesis – PilA-GFP foci of ascospore germlings were less numerous and their distribution was significantly altered, suggesting a correlation between PilA foci and sphingolipid biosynthesis.

1. Introduction

Biological membranes are essential to life and are highly compartmentalized for accomplishing a variety of functions (Simons and Ikonen, 1997). The last decade many studies have focused on the organization of the plasma membrane into space and time. In *Saccharomyces cerevisiae* the plasma membrane contains three types of distinct spatial domains with different lipid and protein composition. W. Tanner and co-workers described MCC (Membrane Compartment of Can1), which harbors at least 19 integral proteins (Young et al., 2002; Malínská et al., 2003), when they observed a "patchy" appearance of the arginine transporter Can1 in the plasma membrane of yeast under normal growth conditions. Another domain formed by the network-like membrane area occupied by Pma1 is called MCP (Membrane Compartment of Pma1) and a third domain contains the target of rapamycin complex 2 (TORC2) called MCT (Malínská et al., 2003; Malinska, 2004; Berchtold and Walther, 2009; Malinsky et al., 2010). MCC organization of the plasma membrane is at least in part mediated by a cellular stable structure termed eisosome, lying underneath MCC patches (Walther et al., 2006). Each eisosome includes three proteins in thousands of copies, the cytoplasmic Pil1 and Lsp1 (Ziółkowska et al., 2012) and the transmembrane protein Sur7. Homologues of Pil1-like proteins are found to be conserved throughout the ascomycetes (Vangelatos et al., 2010). In *S. cerevisiae* eisosomes are organized/regulated by the phosphorylation of Pil1 and Lsp1 by the Pkh1/2 kinase and the levels of sphingolipid long-chain bases (LCBs) (Walther et al., 2007; Luo et al., 2008). Pil1 and the tetra-spanning plasma membrane protein Nce102, which is involved in sensing sphingolipids, are the main organizers of MCC (Frohlich et al., 2009) in *S. cerevisiae*. In their absence, all MCC markers lose their punctate pattern and cells show altered organization of their plasma membrane (Grossmann et al., 2006; Desmyter et al., 2007; Loibl et al., 2010). Both MCC and eisosome components were shown to localize to furrow-like invaginations

* Corresponding author Address: Institute of Biology, National Center for Scientific Research, Demokritos, Aghia Paraskevi 153 10, Athens, Greece. Fax: +30 2106511767.
E-mail address: vicky@bio.demokritos.gr (V. Sophianopoulou).

1087-1845/$ - see front matter © 2013 Elsevier Inc. All rights reserved.
http://dx.doi.org/10.1016/j.fgb.2013.01.002

of the plasma membrane (Strádalová et al., 2009). Recently a comprehensive bioinformatics analysis and structural studies of eisosome proteins in *S. cerevisiae* succeeded in identifying unreported functional domains as well as to demonstrate that eisosome core components Pil1 and Lsp1 belong to the BAR membrane-sculpting superfamily of proteins (Olivera-Couto et al., 2011; Ziółkowska et al., 2012). The type of BAR domains found in Pil1 and Lsp1 were BAR/N-BAR, which act as molecular scaffolds that self-assemble into higher order structures and bind preferentially to PI(4,5)P2 phosphoinositides (Karotki et al., 2011). Overall the available data suggest that eisosome BAR domain components interact with the plasma membrane to generate a specific membrane environment that selects for specific proteins and lipids.

Homologues of Pil1, Lsp1 and Sur7 have been studied in the ascomycetes *Aspergillus nidulans* (Vangelatos et al., 2010), *Candida albicans* (Reijnst et al., 2011), *Ashbya gossypii* (Seger et al., 2011) and *Schizosaccharomyces pombe* (Kabeche et al., 2011). The eisosomal proteins are universally and quite strictly conserved in the subphyla Pezizomycotina and Saccharomycotina, however, this evolutionary conservation is in apparent contradiction with an elusive functional significance (Scazzocchio et al., 2011). Eisosomes were initially proposed to be sites of lipid and protein endocytosis (Walther et al., 2006, 2007), but this function is by no means certain (Alvarez et al., 2008; Grossmann et al., 2008; Brach et al., 2011; Vangelatos et al., 2010). In *Candida albicans*, Sur7 (CaSur7) has additional roles in cell wall synthesis, actin cytoskeleton organization, and septin localization (Alvarez et al., 2008, 2009), while in *S. cerevisiae*, *sur7* mutants show a diminished efficiency of sporulation during cell division (Young et al., 2002; Moreira et al., 2009). In *A. gossypii*, the homologue of Pil1, is very important for polar growth, whereas the homologue of Nce102, which colocalizes with eisosomes is not required for eisosome stability (Seger et al., 2011). In a recent study, fission yeast eisosome protein Pil1 forms filaments that underlie plasma membrane invaginations and generate spatial domains within the cell cortex (Kabeche et al., 2011). Comparative analysis of eisosomes in *S. cerevisiae* and *A. nidulans* reveals striking differences in their assembly and developmental fate (Scazzocchio et al., 2011).

The homothallic fungus *Aspergillus* (*Emericella*) *nidulans* is arguably, among the Pezizomycotina, the organism where membrane proteins have been better studied and is a genetic model system having the ability to reproduce through two different types of spores, conidiospores and ascospores, the products of the asexual and the sexual cycle respectively (Pontecorvo et al., 1953b; Han et al., 2001; Todd et al., 2007). Conidiospores and ascospores are very different cells, which have a radically different morphology and are formed through completely different developmental pathways. Ascospores are formed only after the completion of meiosis inside asci, conidiospores arise from mitotic budding of specialized cells (phialides).

The development of fruiting bodies accompanied by the generation of ascospores is being actively investigated. Ascogenous hyphae fuse to give eventually rise to a large and complex structure, termed the cleistothecium. The cleistothecial wall ('peridium') (Dyer and O'Gorman, 2012) is composed of two layers of dark-purple flattened cells, which at least in *A. nidulans* are glued together with an uncharacterized electron-dense substance ('cleistin') (Champe and Simon, 1992) that fills the intercellular spaces. Large, thick-walled globose cells named hülle cells surround the cleistothecia of *Aspergillus* during development (Carvalho et al., 2002). Hülle cells have a specialized physiology, exhibiting laccase and chitin synthase activity (Hermann et al., 1983), and have been proposed to 'nurse' the cleistothecia during development through the production of α-1,3 glucanase which mobilizes carbon resources required for fruiting body development (Wei et al., 2001). Indeed, it was recently shown that a reduction in the number of hülle cells surrounding ascomata of *A. nidulans* resulted in significantly smaller cleistothecia. In *A. nidulans* an average cleistothecium is the result of a single fertilization event and may contain thousands of asci with eight bi-nucleate, haploid ascospores each arranged in unordered asci (Pontecorvo et al., 1953b; Sohn and Yoon, 2002). Ascospores are released in the environment following the natural breakdown of the ascus wall and the outer wall of the cleistothecium.

We have recently described *A. nidulans* eisosomes (tagging the core proteins PilA, PilB and SurG) during asexual development (asexual spores, conidiophores) and conidial germination (Vangelatos et al., 2010). Moreover, we showed that the Meu14 protein of *Schizosaccharomyces pombe*, necessary for the second division of meiosis and the accurate formation of the forespore membrane (Okuzaki, 2003), is phylogenetically related to Pil1/Pil1A/Lsp1/PilB (22% identity with both Pil1 and PilA, 24% identity with PilB). This work describes the presence and fate of core eisosomal proteins (PilA, PilB and SurG) during ascus development and ascospore germination and also addresses whether the core eisosomal proteins PilA and PilB are necessary for *A. nidulans* sexual cycle progression.

2. Materials and methods

2.1. Media and growth conditions

Minimal (MM) and complete media (CM) as well as the growth conditions for *A. nidulans* were performed as described by Cove (Cove, 1966). When necessary, supplements were added at the adequate concentrations (http://www.fgsc.net/aspergillus/gene_list/supplement.html). Glucose (1%) was used throughout as a carbon source. Urea (5 mM) or ammonium L-(+)-tartrate (10 mM) was used as sole nitrogen source. Myriocin (Sigma–Aldrich) was added in concentrations as indicated and incubated for 3 h or 5 h. Crosses between *A. nidulans* strains were carried out as described by Pontecorvo et al. (1953a) and Todd et al. (2007). Selfing of strains carrying tagged eisosomal proteins was carried out analogously but transferring individual strains to appropriately supplemented minimal or to complete media.

Dehydration experiments were performed as described by Dupont et al., 2010. The solute used in all experiments to perform hyperosmotic treatments was glycerol (Sigma Aldrich). Four conditions were chosen: 1.4 MPa (aw = 0.99), 30 MPa (aw = 0.8), 110 MPa (aw = 0.45) and 166 MPa (aw = 0.3). More particular, selfed cleistothecia of a wild type and the *pilAΔ pilBΔ surGΔ* triple mutant strains were isolated and cleaned by rolling across a 2% agar surface plates. Once clean, cleistotheciae were transferred to an Eppendorf tube containing 30 μL water or 1.4 MPa water–glycerol solution, ruptured, and vortexed to release the ascospores. Ascospores were counted with Haemocytometer, and an equal number of ascospores was placed to 1 mL of different binary water–glycerol solutions (final osmotic pressure of 1.4, 30, 110, or 166 MPa) for rapid perturbations (shock). The cells were maintained for various periods (15 min, 30 min and 1 h at 25 °C) under hyperosmotic conditions before rehydration. Rehydration was rapid, the hyperosmotic solution was removed from the Eppendorf tube after centrifugation (10 min, 5100*g*) and 1 mL of the binary water-glycerol solution (1.4 MPa) was added to the cell pellet. Ascospores' viability was estimated in triplicate by the CFU method. After osmotic treatment, fully rehydrated cells were diluted serially and the appropriate dilutions were plated in MM or CM media. CFUs were counted after 3–5 days of incubation at 25 °C.

2.2. Aspergillus nidulans strains

The different auxotrophic mutations of *A. nidulans* strains are compiled by A.J. Clutterbuck (http://www.gla.ac.uk/acad/ibls/

molgen/aspergillus/index.html). In particular, *pantoB100*, *pabaA1*, *pabaB22*, *riboB2*, *pyroA4*, *pyrG89* and *argB2* indicate auxotrophies for D-pantothenic acid, p-aminobenzoic acid, riboflavin, pyridoxine hydrochloride, uracil/uridine, and L-arginine, respectively. The *nkuA⊿* mutation results in a dramatically decreased frequency of heterologous recombination events into the *A. nidulans* genome (Nayak, 2006). The LO1516 strain expresses functional chimeric histone H1 molecules fused with the monomeric red fluorescent protein (mRFP) (Ramón et al., 2000). These markers do not affect the localization of eisosomal proteins. The VS185 strain was isolated by crossing the MAD1417 with the VS79. The VS151 strain was isolated by crossing the LO1516 with the VS79. The VS199 strain was isolated by crossing the VS48.5 with the VS84. The VS200 strain was isolated by crossing the VS87 with the VS84. VS201 strain was isolated by crossing the VS200 with the VS48.5. All strains used in this work are listed in Table S1. In every case, MM indicates minimal medium supplemented with the requirements relevant to the strains used in the experiment. *pabaA1* was used as a wild-type (wt) strain.

2.3. Reverse transcriptase-PCR

RNA samples were prepared from freshly harvested *A. nidulans* strains. Selfed- cleistothecia were scraped gently from Petri dishes, vortexed gently and vacuum filtered several times using 0.5 mm diameter filters (Durapore®). Cleistothecia were placed on a 3% w/v agar plate and intact cleistothecia were selected microscopically. ~50 mg of cleistothecia were added to a 2.0 mL screw cap Eppendorf tube containing distilled water and crushed using a toothpick to release the ascospores. Ascospores were homogenized in each Eppendorf tube containing 50 mg of glass beads (0.10 mm diameter (Sigma) using the Mini-Beadbeater (BioSpec, Oklahoma, USA) according to the instructions of the manufacturer. RNA was isolated from ungerminated (0 h) and germinated ascospores (12 h) using the TRI Reagent (GIBCO-BRL) kit according to the instructions of the manufacturer. RNA samples were further purified according to the RNeasy Mini Protocol for RNA Cleanup, in the RNeasy Mini Kit (Qiagen) (Bouzarelou et al., 2008). To avoid contamination with genomic DNA, ~10 μg of each RNA sample were treated and cleaned up with TURBO DNA-freeTM kit (Ambion). The absence of DNA contamination was verified with conventional PCRs in which using specific -pilA, pilB, surG and 18S rRNA set of primers, at least 2 μg of each RNA sample as template were amplified for 40 cycles (the absence of products indicates the absence of a detectable DNA contamination under the experimental conditions used). The quality of RNA was confirmed in a conventional 2% w/v agarose gel stained with ethidium bromide (Et-Br) (10 μg/mL). The concentration of each RNA sample was calculated using the nanodrop apparatus (ND-1000 Spectrophotometer) according to the instructions of the manufacturer. Approximately 2 μg of each RNA sample were used for reverse transcription using the SuperScriptTM II RNase H-reverse transcriptase (Invitrogen) according to the instructions of the manufacturer. For semi-quantitative analysis of transcript levels, cDNA was diluted 10-, 100-, 1000-fold. The number of cycles required to produce detectable difference in band intensity between dilutions (to avoid saturation) was determined with Et-Br staining. Densitometry measurements of band intensity, was performed using imageJ software (http://rsb.info.nih.gov/ij/). Experiments were repeated at least three times.

2.4. Total protein extraction and Western blot analysis

For each sample, cleistothecia from 20 Petri dishes were scraped gently, vortexed and vacuum filtered several times using 0.5 mm diameter filters (Durapore®). Approximately 500 mg of ungerminated ascospores (0 h) were frozen and ground in liquid nitrogen. Ascospore powder was resuspended in 1.5 mL ice-cold precipitation buffer (50 mM Tris–HCl pH 7, 50 mM NaCl, 1 mM EDTA) supplemented with a protease inhibitor cocktail (Sigma) and 1 mM phenylmethylsulfonyl fluoride (PMSF). TCA (Trichloroacetic acid) was added (1/8th of the volume) and the suspension was vortexed. After 10 min incubation on ice the suspension was centrifuged for 10 min at 4 °C (15,000*g*). The pellet was washed twice with ice cold acetone, heat-dried and dissolved in 500 μL extraction buffer (150 mM Tris–HCl pH 8, 50 mM NaCl, 1% w/v SDS, 1 mM EDTA and protease inhibitor cocktail (Sigma)). Unbroken cells and larger cell debris were removed by a short, low-speed centrifugation (2000*g* for 2 min). The supernatant was transferred into a new eppendorf and precipitated with TCA as before in 25 μL extraction buffer. Protein samples (25 μL each) were analyzed on a 10% w/v SDS–polyacrylamide gel and electroblotted (Mini Protean Tetra cell; Bio-Rad) onto a polyvinylidene difluoride (PVDF) membrane (Macherey–Nagel) for immunodetection. The membrane was treated with 2% w/v nonfat dry milk, and immunodetection was performed using a primary mouse anti-GFP monoclonal antibody (Roche) and a secondary rabbit anti-mouse IgG horseradish peroxidase (HRP)-linked antibody (Cell Signaling). Blots were developed by the chemiluminescent method using an enhanced chemiluminescence reagent (Amersham Bioscience) and visualized with LAS 4000 (Fuji).

2.5. Microscopy

For analysis of ascospores by laser scanning confocal microscopy (CSLM), the layer of light yellow hülle cells were removed from the black peridium of mature *A. nidulans* cleistothecia (http://www.fgsc.net/fgn48/Kaminskyj.htm) by rolling them on a plate covered with 4% w/v agar. Once clean, the cleistothecium was transferred to an Eppendorf tube containing 20 μL water, crushed and vortexed to release the ascospores. A quantity of 20 μL from a suspension containing 10^5–10^6 ascospores was transferred onto sterile coverslips embedded into appropriate liquid culture media or the suspension was transferred onto sterile microscope slides previously covered with a thin layer of agar medium containing the appropriate nutrient supplements. All samples were incubated for 0–16 h at 25 °C, covered with an oblong large coverglass (22 × 50 size, 13–17 thickness) and subjected to observation by laser scanning confocal microscopy as previously described (Tavoularis et al., 2001, 2003). Cells were imaged by the use of a Leica TCS SP confocal microscope with a Leica PL APO 63x/1.2 NA oil immersion lens. GFP and mRFP were excited with 488 nm and 543 nm laser lines, respectively. Images were acquired sequentially as Z-series (step size 0.5 μm) and processed/analyzed using the Fiji/imagej software (http://imagej.nih.gov/ij/download.html) or the Imaris (Bitplane AG, Zurich, Switzerland). Three dimensional (3D) reconstructions of the ascospores (Fig. S1C) were obtained after isosurface extraction, which converts volume images into geometric surfaces using the 3D visualization software of Imaris.

2.5.1. Quantification of fluorescence signal in captured images

Background noise produced by scatter from out of focus light and by noise inherent to the imaging system was subtracted from cell fluorescence measurements in every experiment using the Image-Pro Plus 6 software, which was also used to quantify fluorescence in the images. Intensity units represent averages of fluorescence signal.

2.5.2. Colocalization analysis

For colocalization assessment images were processed with a median filter to suppress background, and the degree of colocalization is measured by comparing the equivalent pixel positions in

each of the acquired images with the colocalization module of the Imaris software package (Bitplane, Zurich, Switzerland). The colocalization channel – that contains only pixels that represent the co-localization result – was built using Imaris (Bitplane). The Pearson correlation coefficient of channels A (green) and B (red) was used as a measure of the degree of colocalization. Pearson's Correlation is a well defined and commonly accepted means for describing the extent of overlap between image pairs. It is a value computed to be between −1 and 1, with −1 being no overlap and 1 being perfect image colocalization (French et al., 2008). Scatter plots (plotted pixels of a two-channel image) were obtained. In the absence of/low colocalization the scatter plot is bi-lobed as shown in Fig 6, bottom panels, while colocalised pixels are distributed closer to the diagonal of the scatter-plot (upper panels). Additionally the intensities of fluorescent signal in the green and red channels were quantified separately using Imaris (Bitplane) along a line crossing the entire ascospores and their cell cortex and were plotted together (Fig 6 far right panels).

2.5.3. Time-lapse and FRAP experiments

Experiments were conducted at ~26 °C. Cells were imaged by the use of a Leica TCS SP5 confocal microscope with a Leica HCX PL APO CS 63×/1.2 NA water immersion lens. FRAP assays, performed at zoom 3, consisted of three pre-bleach images and four rapid bleach scans at full laser power. Fluorescence loss during the assay due to photobleaching was measured in unbleached regions, averaged and added back to the mean recovery data to correct for photobleaching. The images were analyzed with the Imaris software package (Bitplane, Zurich, Switzerland).

3. Results

3.1. Expression and subcellular localization of eisosomal proteins in hülle cells and asci

During early stages of *A. nidulans* sexual cycle, some hyphae form highly branched structures that become asci and the hülle cells appear (Elliott, 1960). We examined the expression of core eisosomal proteins in strains carrying *pilA-gfp*, *pilB-gfp* and *surG-gfp* alleles and/or single deletions of these alleles during ascus and hülle cells development, using confocal microscopy. These strains also expressed HhoA-mRFP (histone H1-mRFP) protein that labels the nuclei. *A. nidulans* is homothallic. The sexual cycle is induced in laboratory strains of *A. nidulans* by growing the relevant strain or heterokaryon (when crossing two different strains) for 48 h before sealing the plates to lead to conditions of near anaerobiosis. Ascospores/asci were observed 5–7 days after sealing the crossing plates (early, non-pigmented asci, ascospores) and at 14 days after sealing the crossing plates (late, mature asci/ascospores, which were fully pigmented). Our results presented in Fig. 1A–C show that PilA, PilB or SurG are not expressed during the early stages of ascus/ascospore development. No GFP fluorescence was detected in any of the asci/ascospore imaged. PilA, PilB and SurG are expressed and form punctate structures as indicated by the observed fluorescence, in late red-pigmented asci/ascospores (Fig. 1, Fig. S1). To investigate whether the expression of the PilA, PilB and SurG proteins is autonomous, strains expressing PilA-GFP, PilB-GFP and SurG-GFP molecules were crossed with a wild type (*pabaA1*) strain. Ascospores of crossed cleistothecia were observed under an epifluorescence microscope. Each GFP-tagged eisosomal gene segregates 1:1 to the corresponding not labeled wild type gene since approximately half of the ascospores were labeled and half were not (at least 10^3 ascospores derived from a single cleistothecium were counted each time in three independent experiments). Neither PilA, PilB nor SurG are expressed in hülle cells (Fig. 1D–F).

Finally, we detected significant lower expression of histone H1 in early as compared with late ascospores. Whether this represents a genuine difference in the expression or localization of this chromatin protein during the sexual cycle, will be reported separately.

3.2. Subcellular localization of eisosomal proteins during ascospore germination

Polar and equatorial sections of confocal microscopy images of PilA-GFP localization in ungerminated mature ascospores showed a plasma membrane-like punctated staining pattern (Fig. 2). No change in the localization of PilA was seen during the period of ascospore isotropic growth. At the time point of the germ tube emergence and during early polar growth, PilA-GFP is concentrated at the periphery of the ascospore head opposite to the emergent germ tube. In young and mature ascospore-derived germlings, PilA remains mostly restricted to the ascospore head while some PilA spots were detected both at the interior of the hyphae and at its periphery. Similarly, in quiescent ascospores PilB-GFP was also observed to localize at the cell periphery, but it was found to concentrate more at the areas where the two halves of ascospores are joined together (Fig. 3C and D). During the period of isotropic growth as well as after the emergence of the germ tube in young and mature ascospore-derived germlings, PilB-GFP was observed as diffuse fluorescence in the cytoplasm while it was excluded from the nuclei, as shown in a strain carrying both PilB-GFP and the gene encoding histone H1 fused to mRFP (kindly provided by Oakley; Nayak et al., 2006) (Fig. S2A).

Finally, SurG-GFP was localized at both the periphery of ascospores and perinuclearly. This perinuclear location of SurG is seen clearly in a strain carrying both SurG-GFP and the histone H1 gene (HhoA) fused to mRFP (Fig. S2B). During the period of isotropic growth the SurG-GFP perinuclear fluorescence signal diminishes (Fig. 4E and F) and it disappears before the emergence of the germ tube. In ascopore-derived germlings, SurG is confined to the vacuole and endosomes (confirmed by CMAC staining, data not shown) but some residual signal can be detected in the periphery of the ascospore head.

3.3. Core eisosomal genes are expressed during ascospore germination

RT-PCRs in total RNA extracted from ungerminated ascospores (0 h) and ascospore-derived germlings (12 h) of a wild-type strain revealed that mRNAs of both *pilA* and *surG* are abundant throughout the time-interval tested. By contrast *pilB* mRNA is less abundant throughout. The primers used for RT-PCR were expected to produce amplicons of 376 bp (*pilA* cDNA), 286 bp (*pilB* cDNA), 272 bp (*surG* cDNA) and 280 bp (*18S* ribosomal RNA gene) (Fig. 5A). Captured images (Fig. 5D) of ungerminated ascospores (0 h) expressing PilA-, PilB- and SurG- tagged proteins, acquired with the same laser intensity and detector settings, were segmented and fluorescence emission was quantified as mean fluorescence intensity (MFI) with the Image-Pro® Plus software (Fig 5E). Western blots (Fig. 5C) carried out with protein extracts of ungerminated ascospores (0 h), using an anti-GFP monoclonal antibody, showed that bands corresponding to full-length PilA-GFP, PilB-GFP and SurG-GFP proteins are present in ascospores with approximate apparent molecular masses of 70 kDa, 80 kDa and 48 kDa, respectively (calculated molecular mass, 67 kDa 71.5 kDa and 54 kDa respectively). These results indicate that the observed fluorescence corresponds to full-length eisosomal proteins. A band with an apparent molecular mass of 27 kDa corresponding to the proteolytic cleavage of free GFP in the vacuole is seen only in strains carrying the SurG-GFP fusion. These data are consistent with our

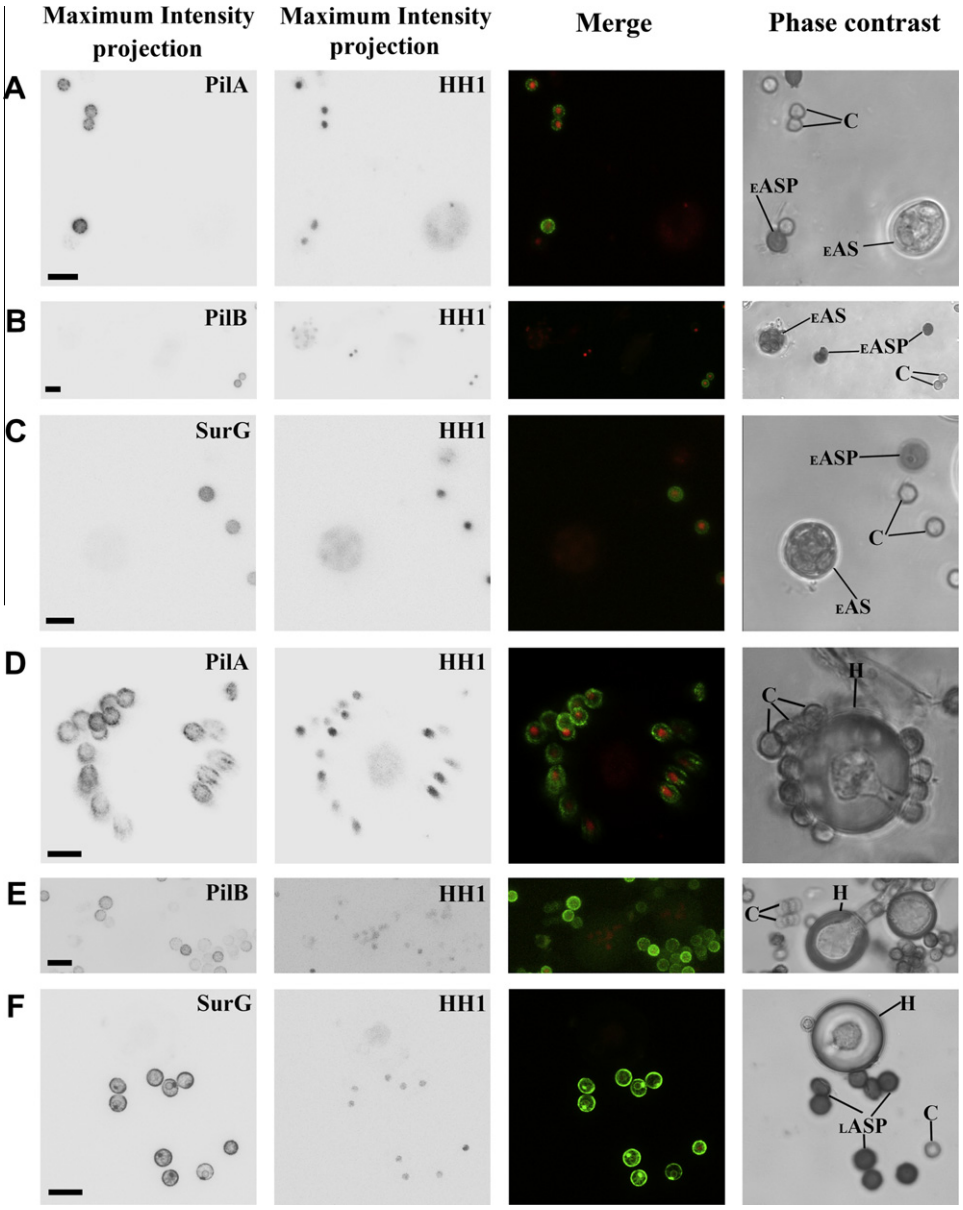

Fig. 1. Expression and subcellular localization of eisosomal proteins during early stages of *A. nidulans* sexual cycle. Maximum-intensity confocal microscopy projections (from optical sections acquired at 0.5 μm intervals) in conidia, early ascospores and early asci of: (A) PilA-GFP and histone H1-mRFP (HH1), (B) PilB-GFP and HH1–mRFP, and (C) SurG-GFP and HH1–mRFP fluorescence. (D–F). The ascospores were obtained by selfing strains VS145, VS151 and VS153 (see Table S1): Maximum-intensity confocal microscopy projections from optical sections acquired at 0.5 μm intervals in hülle cells derived from strains carrying *pilA-gfp*, *pilB-gfp* and *surG-gfp* alleles, respectively. C: conidium; EASP: early ascospore (faint red colored ascospores of 5–7 days cleistothecia); EAS: early ascus (transparent asci in phase contrast images); LASP: late ascospore (dark red pigmented ascospores of 14 days cleistothecia); H: hülle cells. GFP and mRFP fluorescence is shown as inverted gray scale in black and white images. Merged images of fluorescence are shown as colored images. Phase contrast images are shown on the far right column as black and white images. Size bar = 5 μm. (For interpretation of the references to color in this figure legend, the reader is referred to the web version of this article.)

previous findings regarding eisosomal proteins in conidia and conidia-derived germlings (Vangelatos et al., 2010).

3.4. Colocalization of PilA, PilB, and SurG in quiescent ascospores. PilA does not colocalise with endocytic patches

All core eisosomal proteins PilA, PilB and SurG were localized at the periphery of quiescent ascospores. We thus investigated their colocalization. To this aim we used strains carrying PilA-mRFP and PilB-GFP or SurG-GFP molecules. Fig. 6 shows colocalization of PilA with PilB (Pearson's correlation coefficient = 0.77) and colocalisation of PilA with SurG (Pearson's correlation coefficient = 0.89) at the periphery of the ascospores. No colocalization of PilA with the perinuclear fraction of SurG was observed. As we have previously shown by pulse-chase time course experiments using FM4-64, a lipophylic marker of the endocytic pathway (Peñalva, 2005), PilA foci in hyphae do not colocalise with sites of endocytosis (Vangelatos et al., 2010). In this work we reexamined the possible involvement of eisosomes with endocytosis using the AbpA protein (Araujo-Bazán et al., 2008), as a marker for sites of clathrin-mediated endocytosis. AbpA is known to localize predominantly at the hyphal tip and colocalise with actin patches but not with actin cables (Araujo-Bazán et al., 2008). Our results showed that PilA foci do not colocalise with the highly motile and transient peripheral punctate structures of AbpA (Pearson's correlation coefficient = 0.2) (Fig. 6). These results suggest that there is no direct relation between eisosomes and clathrin-mediated endocytosis.

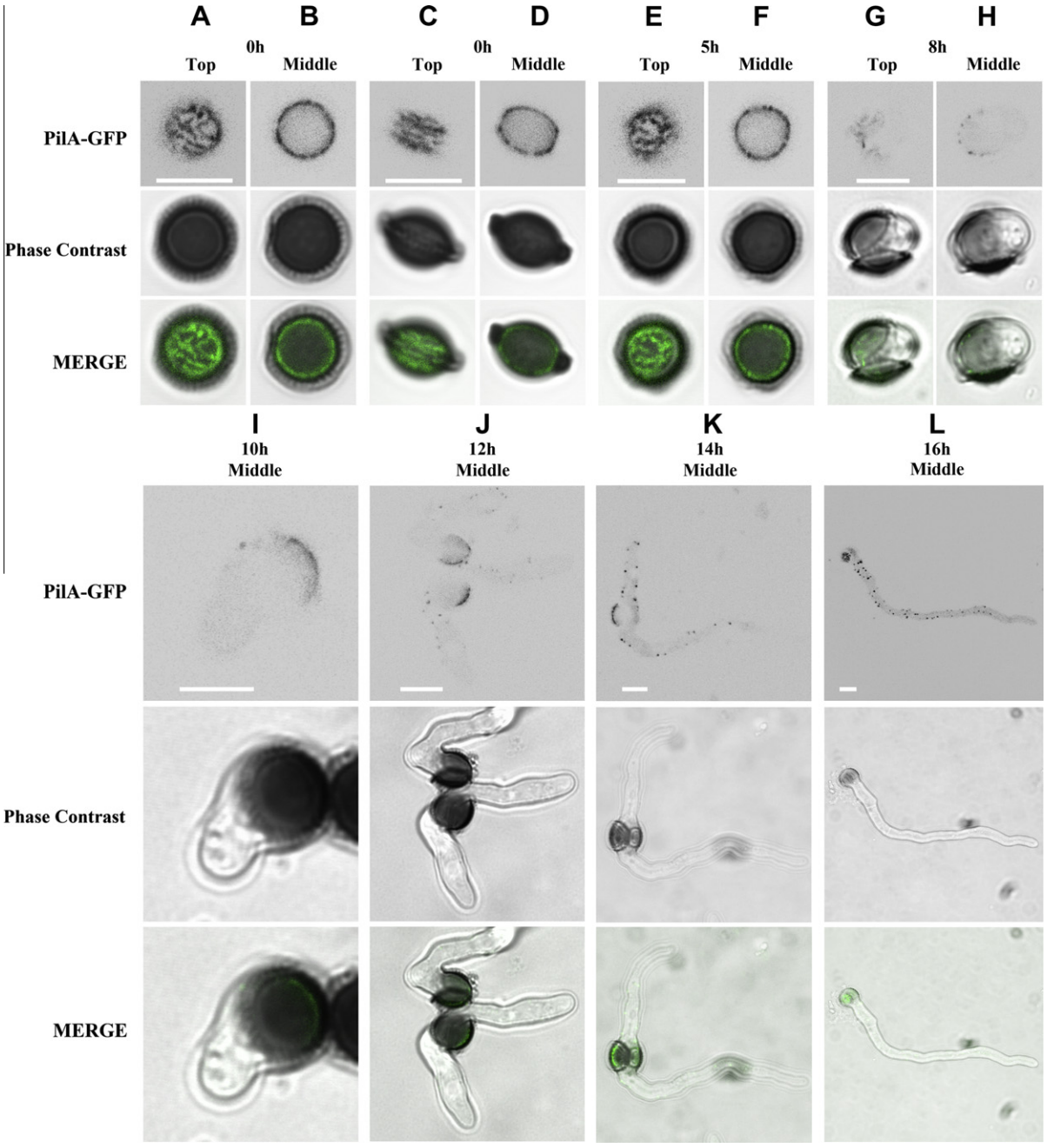

Fig. 2. PilA-GFP localization in ascospores Polar and equatorial sections of ascospores expressing PilA-GFP in (A–D) quiescent ascospores (0 h) oriented parallel to the equatorial plane (A and B) or perpendicular (C and D) to the *xy* plane; (E and F) swollen ascospores (5 h), (G and H) germinated ascospores (8 h). (I–L) equatorial sections of ascospore germlings after 10 h, 12 h, 14 h and 16 h of growth (I–L, respectively). Optical sectioning (step size = 0.5 μm) was performed by confocal microscopy imaging. All fluorescence images were acquired at the same laser intensity and detector settings. Strains were grown in the presence of 5 mM urea and 1% w/v glucose as the sole nitrogen and carbon sources respectively plus supplemented for the relevant auxotrophies, at 25 °C. The ascospores were obtained by selfing strain VS139 (see Table S1). GFP fluorescence is shown as inverted gray scale in black and white images. Phase contrast is shown as black and white images and merged images of fluorescence and phase contrast are shown in color. Size bar = 5 μm. (For interpretation of the references to color in this figure legend, the reader is referred to the web version of this article.)

3.5. PilA forms stable, non mobile structures

We used time-lapse video microscopy and fluorescence recovery after photobleaching (FRAP) techniques to study whether PilA forms static or dynamic structures in ungerminated (0 h) and germinated (12 h) ascospores, quiescent conidia and conidia derived germlings (Fig. 7, Fig. S3). Like Pil1 of fission yeast (Kabeche et al., 2011) and budding yeast (Walther et al., 2006; Alvarez et al., 2008), the PilA-GFP molecules at the membrane of the filamentous *A. nidulans* do not exchange with a cytoplasmic pool fraction, forming stable structures with extremely low mobility (if any), since fluorescence in the bleached area did not recover to any measurable extent over a time period of 20 min.

3.6. Phenotypic characterization of deleted strains

We analyzed the growth characteristics of strains with *pilA*, *pilB*, and *surG* single deletions and a strain carrying a triple deletion of all three core eisosomal genes that we generated in this study (see Section 2). No growth phenotype was seen at 25 °C, 37 °C or 42 °C on either complete or minimal media supplemented with urea, in colonies and germlings derived from ascospores, as

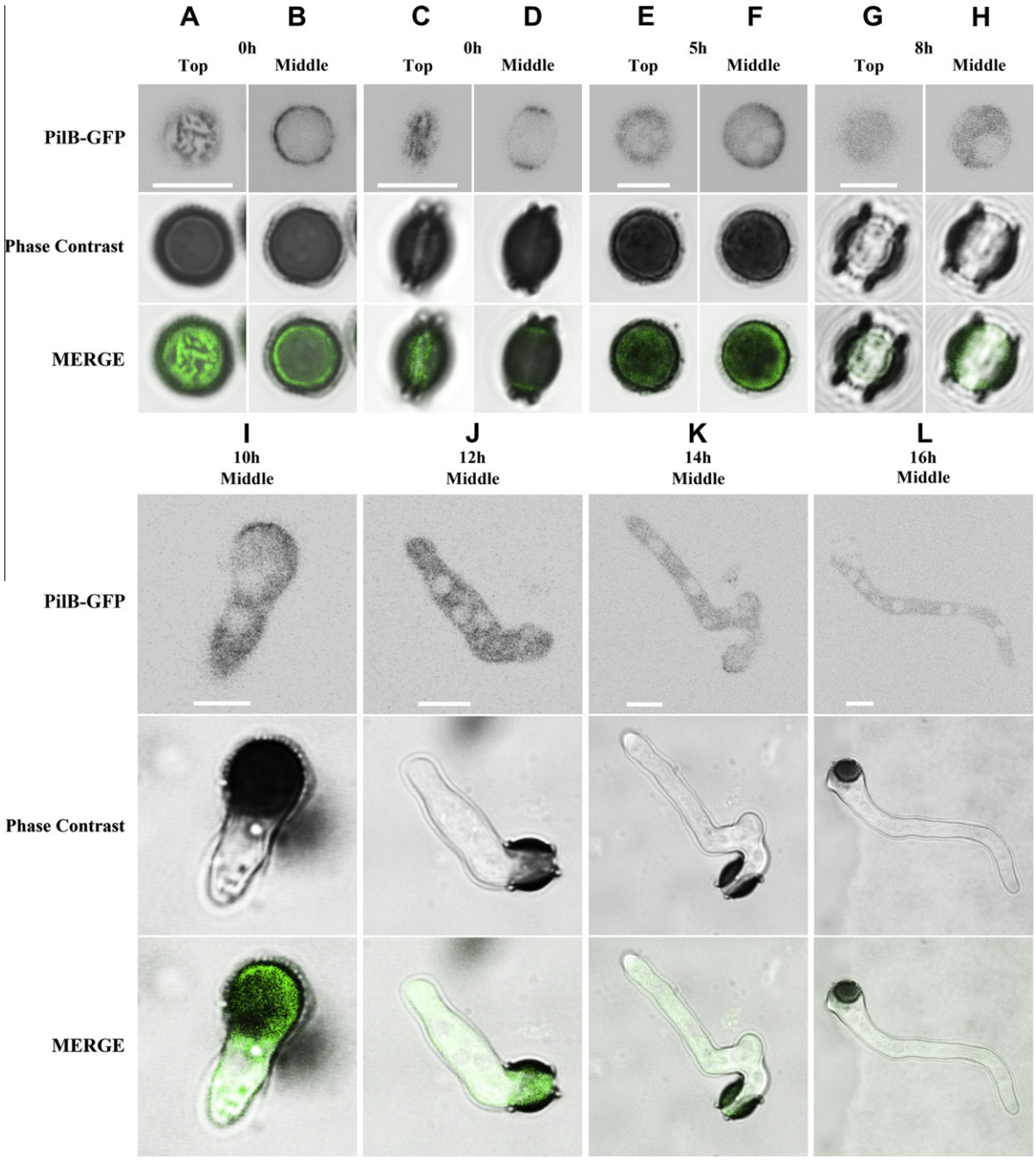

Fig. 3. PilB-GFP localization in ascospores Polar and equatorial sections of ascospores expressing PilB-GFP in (A–D) quiescent ascospores (0 h) oriented parallel with the equatorial plane (A and B) or perpendicular (C and D) to the *xy* plane; (E and F) swollen ascospores (5 h), (G and H) germinated ascospores (8 h). (I–L) equatorial sections of ascospore germlings after 10 h, 12 h, 14 h and 16 h of growth (I–L, respectively). The ascospores were obtained by selfing strain VS138 (see Table S1). Optical sectioning (step size = 0.5 μm) was performed by confocal microscopy imaging. All fluorescence images were acquired at the same laser intensity and detector settings. Strains were grown in the presence of 5 mM urea and 1% w/v glucose as the sole nitrogen and carbon sources respectively, at 25 °C. GFP fluorescence is shown as inverted gray scale in black and white images. Phase contrast in black and white and merged images of fluorescence and phase contrast are shown in color. Size bar = 5 μm. (For interpretation of the references to color in this figure legend, the reader is referred to the web version of this article.)

reported before for colonies derived from asexual spores (Vangelatos et al., 2010). The triple deleted strain was also checked for sensitivity to caffeine, ethanol, SDS, Congo red, osmotic stresses and was found to be indistinguishable from a wild-type strain (data not shown). The ascospores of the triple deleted mutant strain (*pilAΔ pilBΔ surGΔ*) exhibited swelling and polarity establishment (time of germ tube emergence) indistinguishable from that of a wild-type strain at 25 °C, 37 °C or 42 °C (data not shown). We have also examined the viability of the ascospores of the triple mutant strain under rapid dehydration stress conditions, using different binary water-glycerol solutions of final osmotic pressures of 1.4, 30, 110, or 166 MPa, for 15 min, ½ h or 1 h at 25 °C, as described by Dupont et al., 2010. No statistically significant differences of the viability of *pilAΔ pilBΔ surGΔ* and wild-type ascospores was observed under the examined conditions (data not shown).

To investigate whether eisosomes have a role in the sexual cycle of *A. nidulans*, the behavior of single and triple deleted strains was examined in crosses. Our results show that hybrid cleistothecia derived from crosses among strains carrying single *pilA*, *pilB*, and *surG* or double deletions of the eisosome genes contain viable ascospores in which each deleted eisosomal gene segregates 1:1 to the corresponding wild-type gene.

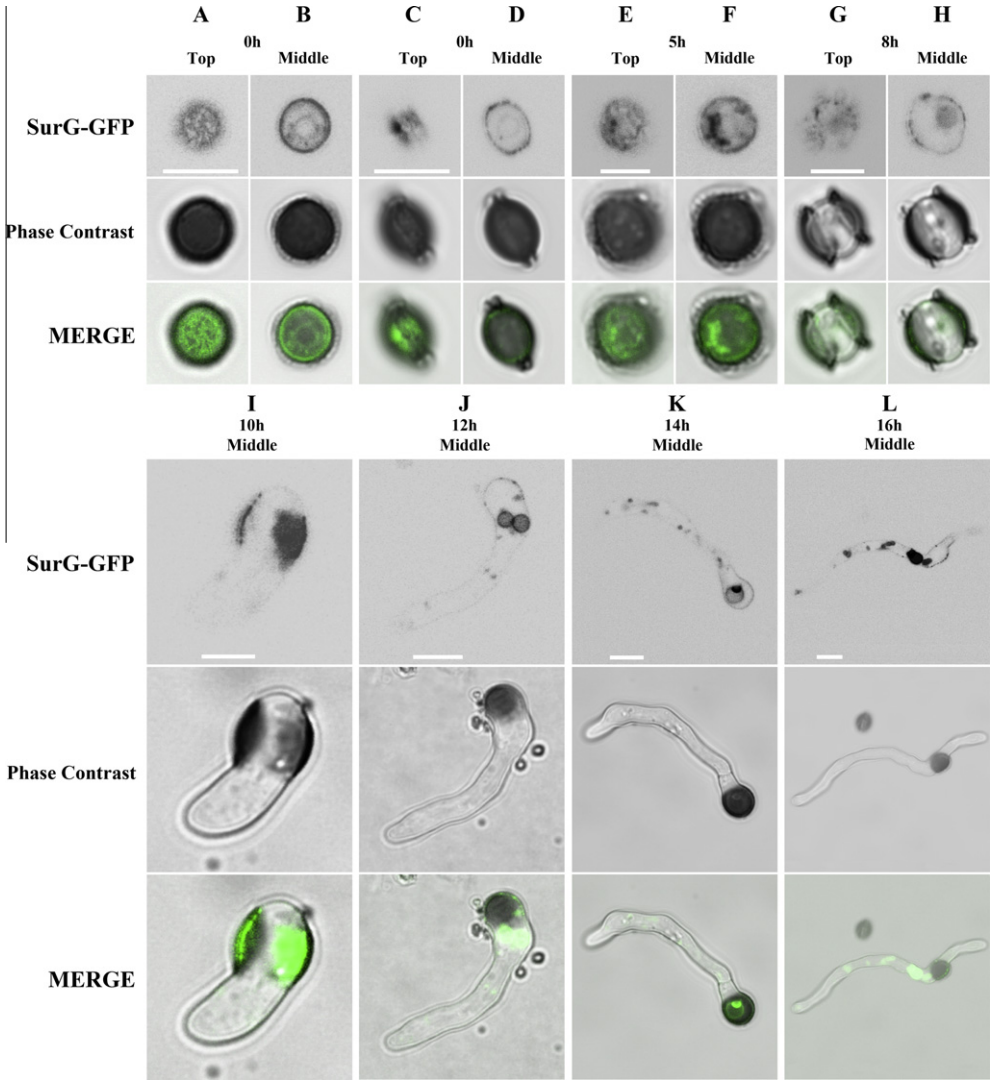

Fig. 4. SurG-GFP localization in ascospores Polar and equatorial sections of ascospores expressing SurG-GFP in (A–D) quiescent ascospores (0 h) oriented parallel with the equatorial plane (A and B) or perpendicular (C and D) to the *xy* plane; (E and F) swollen ascospores (5 h), (G and H) germinated ascospores (8 h). (I–L) equatorial sections of ascospore germlings after 10 h, 12 h, 14 h and 16 h of growth (I–L, respectively). Optical sectioning (step size = 0.5 μm) was performed by confocal microscopy imaging. The ascospores were obtained by selfing strain VS140 (see Table S1). All fluorescence images were acquired at the same laser intensity and detector settings. Strains were grown in the presence of 5 mM urea and 1% w/v glucose as the sole nitrogen and carbon sources respectively, at 25 °C. GFP fluorescence is shown as inverted gray scale in black and white images. Phase contrast in black and white and merged images of fluorescence and phase contrast are shown in color. Size bar = 5 μm. (For interpretation of the references to color in this figure legend, the reader is referred to the web version of this article.)

Moreover, selfed cleistothecia of triple deleted *piAΔ pilBΔ surGΔ* strain or strains carrying single *pilA*, *pilB*, and *surG* deletions contain viable ascospores (~90% viability in respect to the wild-type strain).

Finally, we have checked whether the distribution and the rate of ammonium-elicited endocytosis of the dicarboxylic amino acid transporter AgtA are affected in the triple deleted strain in germinated ascospores. Our results, in agreement with our previous findings concerning the involvement of PilA in ammonium-elicited endocytosis of AgtA in germinated mycelia (Vangelatos et al., 2010), showed no significant alteration of AgtA endocytosis (data not shown).

3.7. PilA localization depends on sphingolipid levels

Experimental observations reported by Frohlich and coworkers in yeast (Frohlich et al., 2009) showed that an MCC protein, Nce102, regulates eisosome biogenesis in response to sphingolipid availability. Myriocin, a widely used specific inhibitor of sphingolipid biosynthesis was chosen to be used in our experiments to create sphingolipid-deficiency (Miyake et al., 1995). After testing various concentrations of myriocin, ranging from 5 μM (1 μg/mL) (as used in *S. cerevisiae* by Frolich et al.) to 80 μg/mL, which is known to affect polarity in *A. nidulans* (Cheng et al., 2001), we chose 20 μg/mL, which is not lethal, as used also by Li et al., 2007. In the presence of this concentration of myriocin we observed delayed growth of *A. nidulans strains* and altered patterns of PilA-GFP distribution. Using the spot detection tool of the Imaris (Bitlane) software we calculated the mean value area of PilA-GFP foci and the number of patches per 20 μm^2 in the presence or absence of myriocin (Fig. C and D). While PilA-GFP is organized in distinct domains distributed all around the surface of ungerminated (0 h) and germinated (12 h) ascospores, in the presence of myriocin, PilA-GFP staining in germinated ascospores was observed in fewer and larger foci (Fig. 8). PilA-GFP had a similar distribution pattern in ungerminated conidia (0 h) (data not shown) and conidia derived germlings (12 h) in the presence of myriocin.

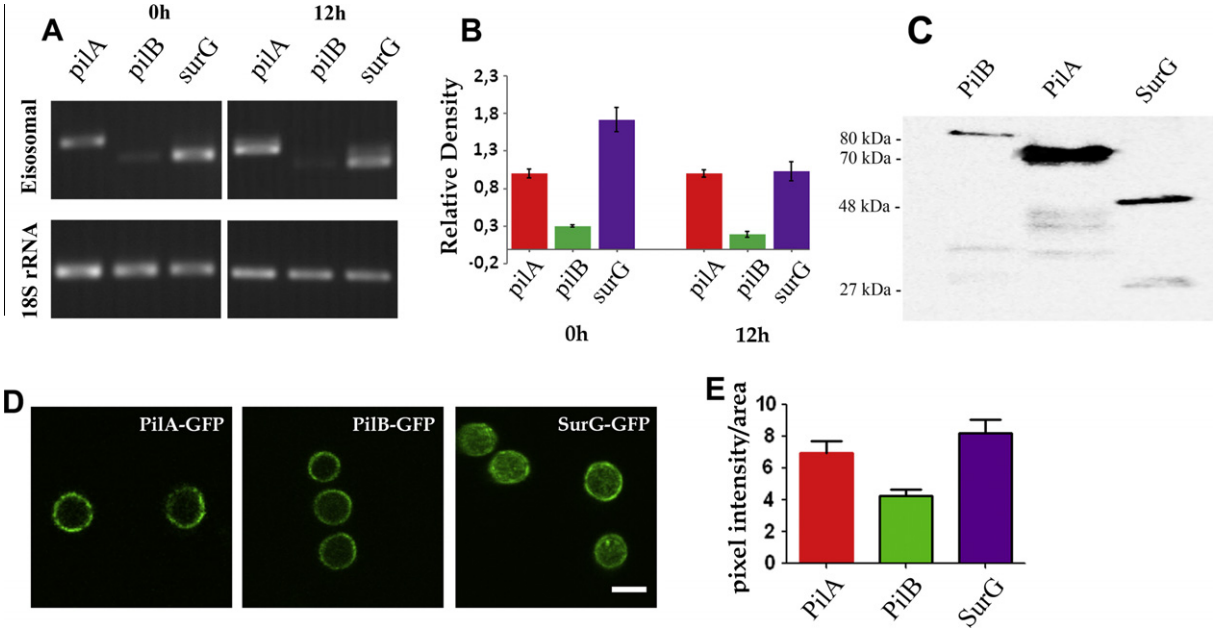

Fig. 5. Expression of core eisosomal genes in ascospores. (A) Expression of *pilA*, *pilB* and *surG* in ungerminated ascospores (0 h) and ascospore germlings (12 h) using semi-quantitative RT-PCRs. (B) Graph presenting the optical density of each amplified band shown in (A) calculated by ImageJ. All values were normalized to the expression of the housekeeping *18S* rRNA gene. (C) Western blot analysis of PilA-, PilB- and SurG-GFP proteins. Approximately 200 μg of total protein fractions of ungerminated ascospores (0 h) from strains expressing PilA, PilB, or SurG proteins tagged with GFP, were separated on a 10% w/v SDS–PAGE, transferred to a PVDF membrane, and probed with a primary mouse anti-GFP monoclonal antibody and a secondary rabbit anti-mouse IgG horseradish peroxidase (HRP)-linked antibody. Protein markers are indicated in kDa on the left. (D) Maximum intensity projections of z-stacks from confocal microscopy images of ungerminated ascospores expressing core eisosomal *GFP*-tagged proteins used for the quantification of the levels of expression of each protein. (E) Graph comparing the levels of expression of the core eisosomal GFP-tagged proteins in ungerminated ascospores based on quantification of the GFP fluorescence in images ($n = 20$) like the ones presented in (D). Pixel values/area were calculated with Image-Pro® Plus software. Size bar = 5 μm. The ascospores were obtained by selfing strains VS138, VS139 and VS140 respectively (see Table S1).

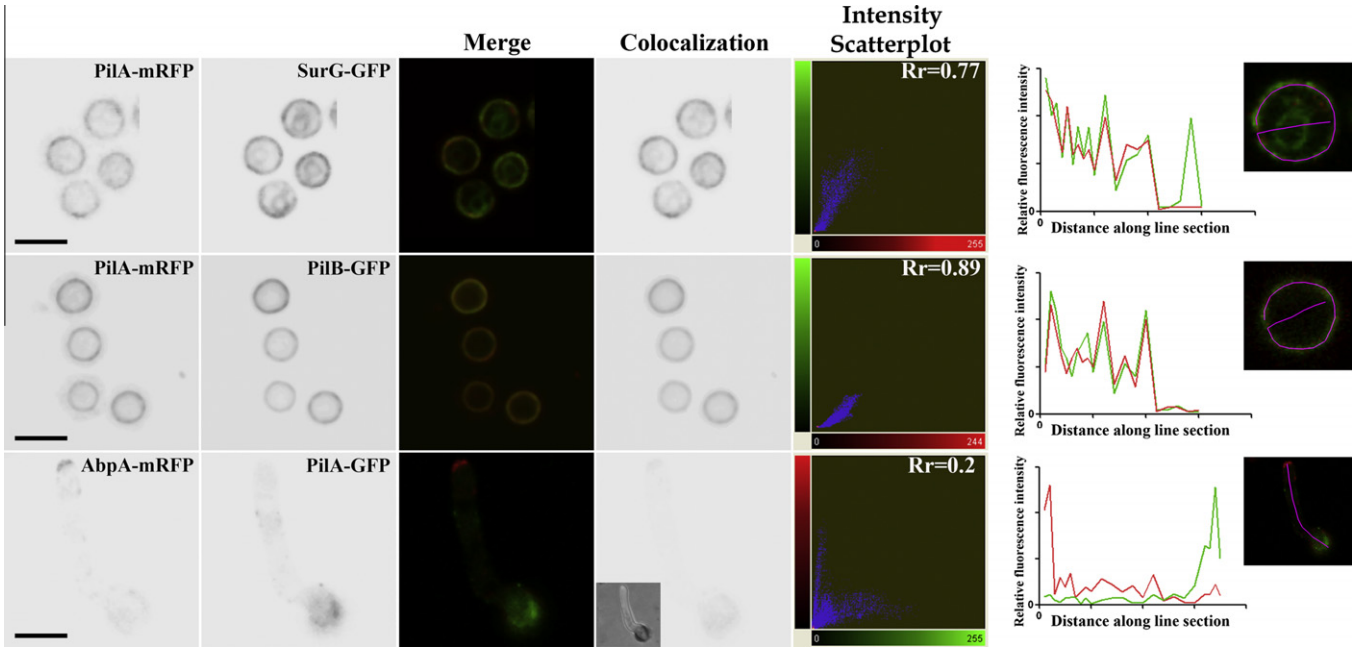

Fig. 6. Colocalization of PilA with PilB and SurG in ungerminated ascospores and PilA with AbpA in ascospore derived hyphae Representative confocal fluorescence images were analyzed after processing with a median filter to suppress background. Corresponding pictures were merged. All pixels colocalised are represented as inverted gray scale images in black and white and scatterplots (fluorogram) pixel intensities are represented with the respective Pearson's correlation coefficients (R_r). The degree of colocalization was determined with the colocalization module of the Imaris software package (Bitplane, Zurich, Switzerland). Analysis of fluorescent intensities along line section is shown in far right panels (see Section 2). The inset in the colocalization image shows a phase contrast image of an optical section. Size bar = 5 μm. The ascospores were obtained by selfing strains VS91, VS94 and VS185 (see Table S1).

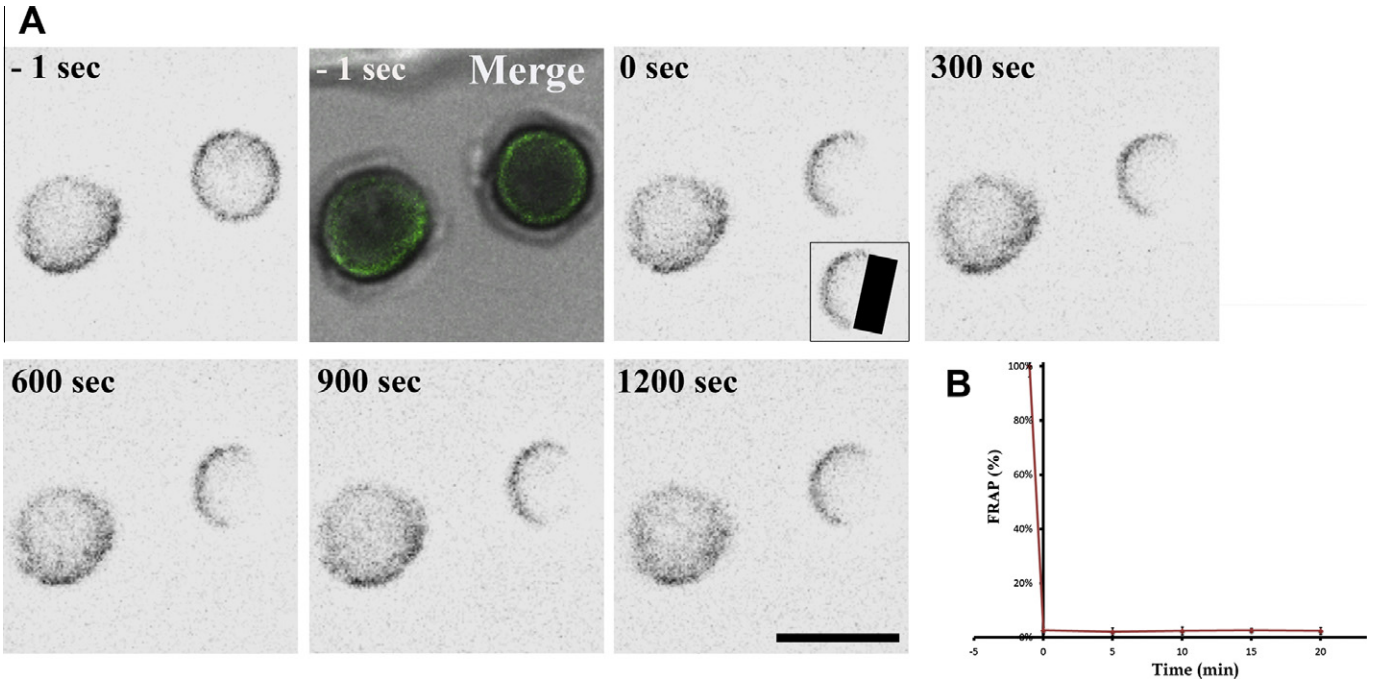

Fig. 7. PilA-GFP molecules form stable structures (A) A representative image of ungerminated ascospores, expressing PilA-GFP, photobleached with a 488 nm laser beam. GFP fluorescence is shown as inverted gray scale in black and white. Merged image of fluorescence and phase contrast is shown in color. The time stated in each panel refers to the time of bleach (0 s). The inset shows the bleached region. (B) Graph showing the fluorescence recovery (%FRAP) in the bleached region over the course of 1200 s (20 min). Size bar = 5 μm. The ascospores were obtained by selfing strain VS139 (see Table S1). (For interpretation of the references to color in this figure legend, the reader is referred to the web version of this article.)

4. Discussion

A. nidulans has a complex sexual cycle that has been studied using morphological, cellular and genetic approaches (Machida and Gomi, 2010 and references therein). One of these approaches is the use of GFP-protein fusions that allow visualization of protein expression during development by fluorescence microscopy. For example, GFP has been used as a tool to monitor the expression of the FcyB cytosine permease in asci of *A. nidulans* (Vlanti and Diallinas, 2008). In the present work we have used biochemical and live cell imaging approaches to study the expression and distribution of the core eisosomal proteins PilA, PilB and SurG in different structures of *A. nidulans* sexual cycle. Our results demonstrate that the three core eisosomal proteins are not expressed either in early and late stages of hülle cells development or during the early stages of ascospore development. They appear as punctate foci at the plasma membrane of quiescent, germinating and germinated ascospores, where their distribution resembles that of conidia (Vangelatos et al., 2010). In contrast to PilA and SurG, we have found that PilB in quiescent ascospores is concentrated where the two halves of the ascospores are joined together. In *S. pombe*, there are two PilA/Pil1-like proteins, Pil1 and Pil2, which are the product of a gene duplication independent to the one which originated PilA and PilB in the Pezizomycotina (Vangelatos et al., 2010). Their distribution in asci is very different from what has been found in either *S. cerevisiae* or *A. nidulans*, Pil1 being restricted to the periphery of the ascus, and Pil2 to the ascospore membrane (Kabeche et al., 2011).

Given that PilA, PilB and SurG are expressed in the sexual cycle of *A. nidulans*, we have examined whether they affect cleistothecium and/or ascospore development. Deletions of each one or all three core eisosomal genes do not affect either ascospore viability or cleistothecium and ascospore morphology. This is in accordance with the fact that *pilA*, *pilB*, and *surG* are expressed late in ascospore development, suggesting that they are not involved in sexual cycle progression. Notwithstanding the presence of eisosomal proteins in mature ascospores their corresponding gene deletions have no obvious effect on ascospore germination in different growth media and temperatures tested.

We have previously reported (Vangelatos et al., 2010) that neither FM4-64 nor the ammonium-elicited endocytosis of the AgtA (dicarboxylic amino acid transporter) are visibly affected in conidia derived germlings of the deleted strains. To further investigate possible involvement of eisosomal proteins in endocytosis, we have tested the possible colocalization of sites of endocytosis and PilA, using the clathrin-mediated endocytosis marker, AbpA (Araujo-Bazán et al., 2008). Our results showed no colocalization of PilA and AbpA. Overall, our data indicate that there is no direct relationship between eisosomes and endocytosis, as also previously reported (Grossmann et al., 2008; Brach et al., 2011).

Time-lapse microscopy and FRAP analysis showed that eisosomes in *A. nidulans* are static as reported previously for eisosomes in *Ashbya gossypii* (Seger et al., 2011) budding yeast (Walther et al., 2006, 2007) and fission yeast (Kabeche et al., 2011). Disruption of sphingolipid biosynthesis by myriocin (an inhibitor of serine palmitoyl transferase) resulted in reduced number of PilA spots and increased cytoplasmic fluorescence compared to myriocin untreated cells. These results are in agreement with experimental observations reported by Frohlich and coworkers in *S. cerevisiae* (Frohlich et al., 2009), who showed that an MCC protein, Nce102, regulates eisosome biogenesis in response to sphingolipid availability. Nce102 regulates kinases pkh1/2, in *S. cerevisiae*, which control eisosome biogenesis through phosphorylation of Pil1 (Frohlich et al., 2009). The orthologues of Nce102 in *A. gossypii* and *Aspergillus fumigatus*, AgNce102 and AfNce102 are functionally divergent, since the AgNce102 is not necessary for eisosome formation while the AfNce102 is required for efficient conidiation and localizes mostly at the ER and the tip of hyphae (Seger et al.,

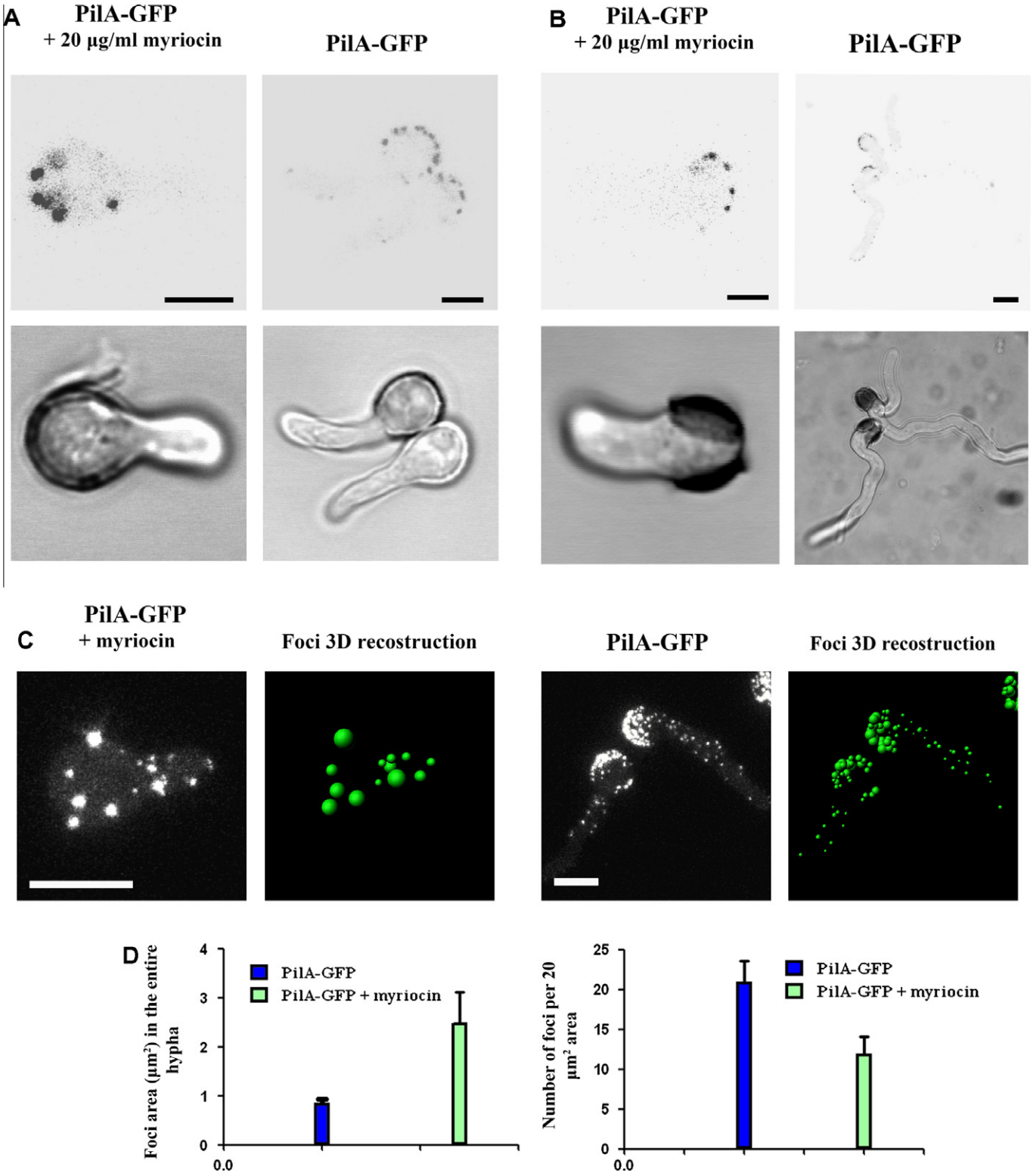

Fig. 8. Effect of myriocin in PilA distribution Equatorial sections of confocal images of a strain expressing PilA-GFP in (A) young mycelia and (B) germinated ascospores (12 h), in the presence of 20 μg/mL myriocin. (C) Images correspond to maximal intensity projections of z-stacks and 3D reconstruction of the same images using spot detection tool of Imaris (Bitlane) of a strain expressing PilA-GFP, in the absence and the presence of 20 μg/mL myriocin. (D) Quantification of PilA foci (mean value area (μm^2) and number of foci per 20 μm^2 area in non-treated and myriocin treated cells. Error bars indicate standard deviations. GFP fluorescence is shown as inverted gray scale in black and white. Corresponding phase contrast images are also shown in black and white at the bottom panels. Size bar = 5 μm. The ascospores were obtained by selfing strain VS139 (see Table S1).

2011; Khalaj et al., 2012). *A. nidulans* also has an orthologue of Nce102 and its role is currently being studied in our laboratory. These results further confirm that the evolutionary conservation of eisosomal proteins in the Ascomycetes is inconsistent with their functional significance. However, a conclusion that can be drawn from the study of core eisosomal proteins in various fungal species

is that eisosome foci are excluded from membrane regions of cell growth (Douglas et al., 2011 and references therein).

Recently, FloA, a protein which localizes at the plasma membrane and is excluded from regions of cell growth, was reported to be implicated in membrane compartmentalization and to play an indirect role in apical sterol-rich plasma membrane domains (SRDs) maintenance (Takeshita et al., 2012). However, FloA is not colocalised with PilA (Athanasopoulos, Gournas and Sophianopoulou unpublished data).

The Sur7 protein of the pathogen *C. albicans* plays a role in morphogenesis, cell wall synthesis and maintenance (Wang et al., 2011 and references therein). Deletion of *SUR7* in *S. cerevisiae* causes defects in sporulation and osmotic stress (Young et al., 2002; Dupont et al., 2010). In contrast, *pilAΔ*, *pilBΔ* and *surGΔ* strains (or triple deleted mutant strain) have not shown any abnormalities in morphogenesis, sporulation, hyphal growth and polarity establishment or any resistance/sensitivity to factors that induce cell wall defects, such as detergents (SDS) and chitin-binding agents (Congo red), suggesting that core eisosomal proteins of *A. nidulans* are not playing any indirect/direct role in cell wall synthesis/maintenance. Moreover, deletion of *sur7* in *C. albicans* results in marked hypersensitivity to fluconazoles (Alvarez et al., 2008), a triazole antifungal agent which is an inhibitor of ergosterol biosynthesis, to which *A. nidulans* is tolerant (Edlind and Katiyar, 2004). Interestingly, deletion of either or both *surG* and *pilA* genes lead to moderate resistance to another antifungal triazole agent, itraconazole (Vangelatos et al., 2010). Overall, despite differences in temporal expression and membrane distribution of core eisosome proteins in different fungi, the types of different structures – puncta or filaments (Kabeche et al., 2011) – eisosomes form, all available data implicate eisosomal proteins in plasma membrane (PM) organization. The importance of plasma membrane organization is highlighted by the fact that the most effective antifungal drugs, target lipids and proteins in this essential barrier. Future studies will contribute to elucidate the mechanisms involved in eisosomes assembly/disassembly, understanding their function in different fungal species and hopefully comprehend the relationship between PM organization and pathogenicity. Notwithstanding the elusive function of eisosomal proteins, it is noteworthy that the distribution in ascospores and conidiospores, quiescent, long-term survival cells, that have a quite different developmental origin, is almost identical, and quite different from that in growing germlings and mycelia.

Acknowledgments

We thank I. Vangelatos who obtained preliminary data on the presence of eisosomes in ascospores. Most of the Imaging work was performed at the Light microscopy unit of the Hellenic Pasteur Institute (LMU-HPI). The FRAP and Time-lapse experiments were performed at the Biological Imaging Unit of the Biomedical Research Foundation (BIU-BRF) in Athens Greece. The authors acknowledge the technical assistance of Dr. Evagelia Xingi (LMU-HPI) and Dr. Eleni Rigana (BIU-BRF) in the imaging experiments. We thank Prof. B.R. Oakley for the mRFP-H1 containing strain and Dr. M. Peñalva for the AbpA-mRFP containing strain. We also thank Dr. G. Diallinas and Dr. C. Gournas for critical reading of the manuscript. This work was supported by research grant from the NCSR Demokritos to A. A.

Appendix A. Supplementary material

Supplementary data associated with this article can be found, in the online version, at http://dx.doi.org/10.1016/j.fgb.2013.01.002.

References

Alvarez, F.J., Douglas, L.M., Konopka, J.B., 2009. The Sur7 protein resides in punctate membrane subdomains and mediates spatial regulation of cell wall synthesis in *Candida albicans*. Communicative & Integrative Biology 2, 76–77.

Alvarez, F.J., Douglas, L.M., Rosebrock, A., Konopka, J.B., 2008. The Sur7 protein regulates plasma membrane organization and prevents intracellular cell wall growth in *Candida albicans*. Molecular Biology of the Cell 19, 5214–5225.

Araujo-Bazán, L., Peñalva, M.A., Espeso, E.A., 2008. Preferential localization of the endocytic internalization machinery to hyphal tips underlies polarization of the actin cytoskeleton in *Aspergillus nidulans*. Molecular Microbiology 67, 891–905.

Berchtold, D., Walther, T.C., 2009. TORC2 plasma membrane localization is essential for cell viability and restricted to a distinct domain. Molecular Biology of the Cell 20, 1565–1575.

Bouzarelou, D., Billini, M., Roumelioti, K., Sophianopoulou, V., 2008. EglD, a putative endoglucanase, with an expansin like domain is localized in the conidial cell wall of *Aspergillus nidulans*. Fungal Genetics and Biology: FG & B 45, 839–850.

Brach, T., Specht, T., Kaksonen, M., 2011. Reassessment of the role of plasma membrane domains in the regulation of vesicular traffic in yeast. Journal of Cell Science 124, 328–337.

Carvalho, M.D.F., Baracho, M.S., Baracho, I.R., 2002. An investigation of the nuclei of hülle cells of *Aspergillus nidulans*. Genetics and Molecular Biology 25, 485–488.

Champe, S.P., Simon, L.D., 1992. Cellular differentiation and tissue formation in the fungus *Aspergillus nidulans*. In: Rossomando, E.F., Alexander, S. (Eds.), Morphogenesis: an analysis of the development of biological form. Dekker, New York, NY, pp. 63–91.

Cheng, J., Park, T.-S., Fischl, A.S., Ye, X.S., 2001. Cell cycle progression and cell polarity require sphingolipid biosynthesis in *Aspergillus nidulans*. Molecular and Cellular Biology 21, 6198–6209.

Cove, D.J., 1966. The induction and repression of nitrate reductase in the fungus *Aspergillus nidulans*. Biochimica et Biophysica Acta 113, 51–56.

Desmyter, L., Verstraelen, J., Dewaele, S., Libert, C., Contreras, R., Chen, C., 2007. Nonclassical export pathway: overexpression of NCE102 reduces protein and DNA damage and prolongs lifespan in an SGS1 deficient *Saccharomyces cerevisiae*. Biogerontology 8, 527–535.

Douglas, L.M., Wang, H.X., Li, L., Konopka, J.B., 2011. Membrane compartment occupied by Can1 (MCC) and eisosome subdomains of the fungal plasma membrane. Membranes 1, 394–411.

Dupont, S., Beney, L., Ritt, J.-F., Lherminier, J., Gervais, P., 2010. Lateral reorganization of plasma membrane is involved in the yeast resistance to severe dehydration. Biochimica et Biophysica Acta (BBA) – Biomembranes 1798, 975–985.

Dyer, P.S., O'Gorman, C.M., 2012. Sexual development and cryptic sexuality in fungi: insights from *Aspergillus* species. FEMS Microbiology Reviews 36, 165–192.

Edlind, T.D., Katiyar, S.K., 2004. The echinocandin 'target' identified by cross-linking is a homolog of Pil1 and Lsp1, sphingolipid-dependent regulators of cell wall integrity signaling. Antimicrobial Agents and Chemotherapy 48, 4491.

Elliott, C.G., 1960. The cytology of *Aspergillus nidulans*. Genetics Research 1, 462–476.

French, A.P., Mills, S., Swarup, R., Bennett, M.J., Pridmore, T.P., 2008. Colocalization of fluorescent markers in confocal microscope images of plant cells. Nature Protocols 3, 619–628.

Frohlich, F., Moreira, K., Aguilar, P.S., Hubner, N.C., Mann, M., Walter, P., Walther, T.C., 2009. A genome-wide screen for genes affecting eisosomes reveals Nce102 function in sphingolipid signaling. The Journal of Cell Biology 185, 1227–1242.

Grossmann, G., Malinsky, J., Stahlschmidt, W., Loibl, M., Weig-Meckl, I., Frommer, W.B., Opekarová, M., Tanner, W., 2008. Plasma membrane microdomains regulate turnover of transport proteins in yeast. The Journal of Cell Biology 183, 1075–1088.

Grossmann, G., Opekarová, M., Malinsky, J., Weig-Meckl, I., Tanner, W., 2006. Membrane potential governs lateral segregation of plasma membrane proteins and lipids in yeast. The EMBO Journal 26, 1–8.

Han, K.H., Han, K.Y., Yu, J.H., Chae, K.S., Jahng, K.Y., Han, D.M., 2001. The nsdD gene encodes a putative GATA-type transcription factor necessary for sexual development of *Aspergillus nidulans*. Molecular microbiology 41, 299–309.

Hermann, T.E., Kurtz, M.B., Champe, S.P., 1983. Laccase localized in hulle cells and cleistothecial primordia of *Aspergillus nidulans*. Journal of Bacteriology 154, 955–964.

Kabeche, R., Baldissard, S., Hammond, J., Howard, L., Moseley, J.B., 2011. The filament-forming protein Pil1 assembles linear eisosomes in fission yeast. Molecular Biology of the Cell 22, 4059–4067.

Karotki, L., Huiskonen, J.T., Stefan, C.J., Ziółkowska, N.E., Roth, R., Surma, M.A., Krogan, N.J., Emr, S.D., Heuser, J., Grünewald, K., Walther, T.C., 2011. Eisosome proteins assemble into a membrane scaffold. The Journal of Cell Biology 195, 889–902.

Khalaj, V., Azizi, M., Enayati, S., Khorasanizadeh, D., Ardakani, E.M., 2012. NCE102 homologue in *Aspergillus fumigatus* is required for normal sporulation, not hyphal growth or pathogenesis. FEMS Microbiology Letters 329, 138–145.

Li, S., Bao, D., Yuen, G., Harris, S.D., Calvo, A.M., 2007. BasA Regulates Cell Wall Organization and Asexual/Sexual Sporulation Ratio in *Aspergillus nidulans*. Genetics 176, 243–253.

Loibl, M., Grossmann, G., Stradalova, V., Klingl, A., Rachel, R., Tanner, W., Malinsky, J., Opekarova, M., 2010. C terminus of Nce102 determines the structure and function of microdomains in the *Saccharomyces cerevisiae* plasma membrane. Eukaryotic Cell 9, 1184–1192.

Luo, G., Gruhler, A., Liu, Y., Jensen, O.N., Dickson, R.C., 2008. The sphingolipid long-chain base-Pkh1/2-Ypk1/2 signaling pathway regulates eisosome assembly and turnover. Journal of Biological Chemistry 283, 10433–10444.

Machida, M., Gomi, K., 2010. Molecular Biology and Genomics. Horizon Scientific Press, Aspergillus.

Malinska, K., 2004. Distribution of Can1p into stable domains reflects lateral protein segregation within the plasma membrane of living *S. cerevisiae* cells. Journal of Cell Science 117, 6031–6041.

Malínská, K., Malínsk, J., Opekarová, M., Tanner, W., 2003. Visualization of protein compartmentation within the plasma membrane of living yeast cells. Molecular Biology of the Cell 14, 4427–4436.

Malinsky, J., Opekarová, M., Tanner, W., 2010. The lateral compartmentation of the yeast plasma membrane. Yeast 27, 473–478.

Miyake, Y., Kozutsumi, Y., Nakamura, S., Fujita, T., Kawasaki, T., 1995. Serine palmitoyltransferase is the primary target of a sphingosine-like immunosuppressant, ISP-1/myriocin. Biochemical and Biophysical Research Communications 211, 396–403.

Moreira, K.E., Walther, T.C., Aguilar, P.S., Walter, P., 2009. Pil1 controls eisosome biogenesis. Molecular Biology of the Cell 20, 809–818.

Nayak, T., 2006. A versatile and efficient gene-targeting system for *Aspergillus nidulans*. Genetics 172, 1557–1566.

Okuzaki, D., 2003. Fission yeast meu14+ is required for proper nuclear division and accurate forespore membrane formation during meiosis II. Journal of Cell Science 116, 2721–2735.

Olivera-Couto, A., Graña, M., Harispe, L., Aguilar, P.S., 2011. The eisosome core is composed of BAR domain proteins. Molecular Biology of the Cell 22, 2360–2372.

Peñalva, M.A., 2005. Tracing the endocytic pathway of *Aspergillus nidulans* with FM4-64. Fungal Genetics and Biology 42, 963–975.

Pontecorvo, G., Roper, J.A., Chemmons, L.M., Macdonald, K.D., Bufton, A.W.J., 1953a. The genetics of *Aspergillus nidulans*. In: Advances in Genetics. Elsevier. pp. 141–238.

Pontecorvo, G., Roper, J.A., Hemmons, L.M., Macdonald, K.D., Bufton, A.W.J., 1953b. The genetics of Aspergillus nidulans. Advances in Genetics 5, 141–238.

Ramón, A., Muro-Pastor, M.I., Scazzocchio, C., Gonzalez, R., 2000. Deletion of the unique gene encoding a typical histone H1 has no apparent phenotype in *Aspergillus nidulans*. Molecular Microbiology 35, 223–233.

Reijnst, P., Walther, A., Wendland, J., 2011. Dual-colour fluorescence microscopy using yEmCherry-/GFP-tagging of eisosome components Pil1 and Lsp1 in Candida albicans. Yeast (Chichester, England) 28, 331–338.

Scazzocchio, C., Vangelatos, I., Sophianopoulou, V., 2011. Eisosomes and membrane compartments in the ascomycetes: a view from *Aspergillus nidulans*. Communicative & Integrative Biology 4, 64.

Seger, S., Rischatsch, R., Philippsen, P., 2011. Formation and stability of eisosomes in the filamentous fungus *Ashbya gossypii*. Journal of Cell Science 124, 1629–1634.

Simons, K., Ikonen, E., 1997. Functional rafts in cell membranes. Nature 387, 569–572.

Sohn, K.T., Yoon, K.S., 2002. Ultrastructural study on the cleistothecium development in *Aspergillus nidulans*. Mycobiology 30, 117–127.

Strádalová, V., Stahlschmidt, W., Grossmann, G., Blazíková, M., Rachel, R., Tanner, W., Malinsky, J., 2009. Furrow-like invaginations of the yeast plasma membrane correspond to membrane compartment of Can1. Journal of Cell Science 122, 2887–2894.

Takeshita, N., Diallinas, G., Fischer, R., 2012. The role of flotillin FloA and stomatin StoA in the maintenance of apical sterol-rich membrane domains and polarity in the filamentous fungus *Aspergillus nidulans*. Molecular Microbiology 83, 1136–1152.

Tavoularis, S., Scazzocchio, C., Sophianopoulou, V., 2001. Functional expression and cellular localization of a green fluorescent protein-tagged proline transporter in *Aspergillus nidulans*. Fungal Genetics and Biology 33, 115–125.

Tavoularis, S.N., Tazebay, U.H., Diallinas, G., Sideridou, M., Rosa, A., Scazzocchio, C., Sophianopoulou, V., 2003. Mutational analysis of the major proline transporter (PrnB) of *Aspergillus nidulans*. Molecular Membrane Biology 20, 285–297.

Todd, R.B., Davis, M.A., Hynes, M.J., 2007. Genetic manipulation of *Aspergillus nidulans*: meiotic progeny for genetic analysis and strain construction. Nature Protocols 2, 811–821.

Vangelatos, I., Roumelioti, K., Gournas, C., Suarez, T., Scazzocchio, C., Sophianopoulou, V., 2010. Eisosome organization in the filamentous ascomycete *Aspergillus nidulans*. Eukaryotic Cell 9, 1441–1454.

Vlanti, A., Diallinas, G., 2008. The *Aspergillus nidulans* FcyB cytosine-purine scavenger is highly expressed during germination and in reproductive compartments and is downregulated by endocytosis. Molecular Microbiology 68, 959–977.

Walther, T.C., Aguilar, P.S., Fröhlich, F., Chu, F., Moreira, K., Burlingame, A.L., Walter, P., 2007. Pkh-kinases control eisosome assembly and organization. The EMBO Journal 26, 4946–4955.

Walther, T.C., Brickner, J.H., Aguilar, P.S., Bernales, S., Pantoja, C., Walter, P., 2006. Eisosomes mark static sites of endocytosis. Nature 439, 998–1003.

Wang, H.X., Douglas, L.M., Aimanianda, V., Latgé, J.-P., Konopka, J.B., 2011. The *Candida albicans* Sur7 protein is needed for proper synthesis of the fibrillar component of the cell wall that confers strength. Eukaryotic cell 10, 72–80.

Wei, H., Scherer, M., Singh, A., Liese, R., Fischer, R., 2001. *Aspergillus nidulans* alpha-1,3 glucanase (mutanase), mutA, is expressed during sexual development and mobilizes mutan. Fungal Genetics and Biology: FG & B 34, 217–227.

Young, M.E., Karpova, T.S., Brügger, B., Moschenross, D.M., Wang, G.K., Schneiter, R., Wieland, F.T., Cooper, J.A., 2002. The Sur7p family defines novel cortical domains in *Saccharomyces cerevisiae*, affects sphingolipid metabolism, and is involved in sporulation. Molecular and cellular biology 22, 927–934.

Ziółkowska, N.E., Christiano, R., Walther, T.C., 2012. Organized living: formation mechanisms and functions of plasma membrane domains in yeast. Trends in Cell Biology 22, 151–158.